Active intraplate strike-slip faulting and transpressional uplift in the Mongolian Altai

D. CUNNINGHAM[1], A. DIJKSTRA[1], J. HOWARD[1], A. QUARLES[2] & G. BADARCH[3]

[1]*Orogenic Processes Group, Department of Geology, University of Leicester, Leicester, UK (e-mail: wdc2@le.ac.uk)*

[2]*2304 Forest Hills Rd, Grapevine, Texas, USA*

[3]*Institute of Geology and Mineral Resources, Mongolian Academy of Sciences, Ulaan Baatar, Mongolia*

Abstract: The Mongolian Altai is a Late Cenozoic intraplate strike-slip deformation belt which formed as a distant strain response to the Indo-Eurasian collision over 2000 km to the south. We report results from 5 weeks of detailed fieldwork carried out during summer 2000 in northwestern Mongolia investigating the crustal architecture of the Altai at latitude 48°N. The region can be divided into discrete Cenozoic structural domains each dominated by a major dextral strike-slip fault system or range-bounding thrust fault. Gentle bends along the major strike-slip faults are marked by transpressional uplifts including asymmetric thrust ridges, restraining bends, and triangular thrust-bounded massifs. These transpressional uplifts (Tsambagarav Massif, Altun Huhey Uul, Sair Uul, Hoh Serhiyn Nuruu, Omno Hayrhan Uula, Mengildyk Nuruu) comprise the highest mountains in the Mongolian Altai and are structural and metamorphic culminations exposing polydeformed greenschist–amphibolite grade basement recording at least two phases of Palaeozoic ductile deformation overprinted by Cenozoic brittle structures. Cenozoic thrust faults with the greatest amounts of displacement bound the W and SW sides of ranges throughout the region and consistently verge WSW. Each major range is essentially a NE-tilted block and this is reflected by asymmetric internal drainage patterns. Many faults are considered active because they deform surficial deposits, form prominent scarps, and define range fronts with low sinuosity where active alluvial fan deposition takes place. Reactivation of the prevailing NW-striking, NE-dipping Palaeozoic basement anisotropy is a regionally important control on the orientation and kinematics of Cenozoic faults. At first order, the Altai is spatially partitioned into a low-angle thrust belt that overthrusts the Junggar Basin on the Chinese side and a high-angle SW-vergent dextral transpressional belt on the Mongolian side. The mechanically rigid Hangay craton and Junggar basement block which bound the Altai on either side have played a major role in focusing Late Cenozoic deformation along their boundaries and within the Altai. The geometric relationship between rigid block boundaries, Palaeozoic basement structural anisotropy, and the dominantly NE SHmax (derived from India's continued NE indentation) has dictated the kinematics of Late Cenozoic deformation in the Altai, Gobi Altai, and Sayan regions.

The Altai is one of the great intraplate mountain ranges of central Asia extending over 1700 km from Siberia to the Gobi Desert (Fig. 1). The range is tectonically active and cut by regional-scale strike-slip faults characterized by dextral transpressional deformation (Cunningham *et al.* 1996; Cunningham 1998). These faults have produced several large historical earthquakes (M = 7+) with impressive ground rupturing (Khil'ko *et al.* 1985; Trifonov 1988; Baljinnyam *et al.* 1993; Bayasgalan *et al.* 1999). Late Cenozoic faulting and uplift of the Altai is believed to be ultimately driven by NE-directed compressional stresses derived from the Indo-Eurasian collision over 2000 km to the south (Tapponnier & Molnar 1979; Baljinnyam *et al.* 1993; Cunningham *et al.* 1996). Compared to the Himalayas, Karakorum, Pamirs, Tibet, and Tien Shan, the Altai has received much less attention from workers investigating the effects of the Indo-Eurasia collision. This is presumably because the Altai is more distant and has accommodated less total Cenozoic strain. Nevertheless, the Altai is particularly interesting to structural geologists interested in transpressional deformation because the range is less overprinted by contractional structures than major ranges to the south, and the linkage between strike-slip faults and thrust and oblique-slip faults is spectacularly exposed. Thus

From: STORTI, F., HOLDSWORTH, R. E. & SALVINI, F. (eds) *Intraplate Strike-Slip Deformation Belts*. Geological Society, London, Special Publications, **210**, 65–87, 0305-8719/03/$15

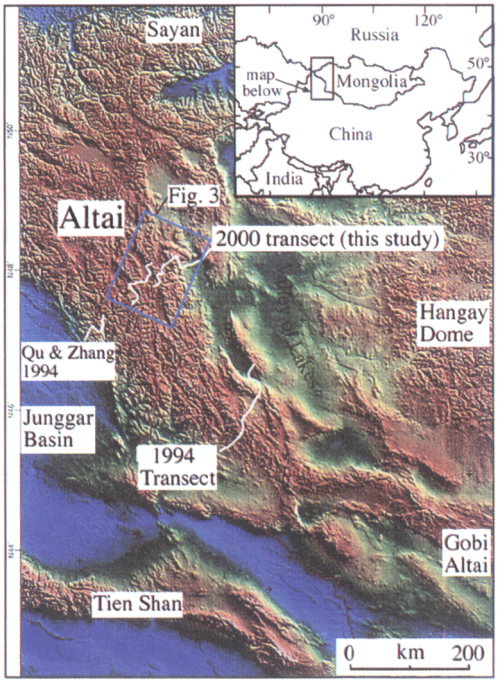

Fig. 1. Digital topographic map of Altai region and area investigated in this study. Location of Landsat image shown in Figure 3 is also indicated.

the Altai is one of the best places in the world to study the evolutionary development and internal architecture of an active intraplate strike-slip deformation belt.

We carried out 5 weeks of fieldwork in the Mongolian Altai region during the summer of 2000 (Fig. 1) investigating the cross-strike structure of the range from east to west in order to better understand overall processes of Cenozoic intracontinental mountain building and the distant effects of the Indo-Eurasia collision. From a modern structural geology standpoint, the Altai remains one of the least studied major mountain ranges on Earth and the first-order crustal architecture of the range has never before been documented. Our study complements a detailed transect completed in 1994 further south by Cunningham *et al.* (1996) and was chosen to link with a structural section completed by Qu and Zhang (1994) through the Chinese Altai (Fig. 1). In keeping with the theme of this volume, we focus here specifically on the active transpressional deformation associated with Cenozoic intraplate strike-slip faulting in the Altai region (Figs 1, 2). Detailed information on the Palaeozoic evolution of the basement rocks is beyond the scope of this paper and is being prepared as a separate manuscript for submission elsewhere.

The physiography of the Altai reflects tectonic and climatic controls. The western and northwestern Altai region in China, Russia, and Kazakhstan receives the most precipitation, is more incised by rivers, and is covered by forest. To the east and south in Mongolia, the range is in a rain shadow and is more arid with less river incision, better preserved summit peneplains and less permanent snow. For this reason, space views of the Altai give the impression that the Chinese Altai is topographically highest because it contains more rugged snow-covered mountains. However, the Mongolian Altai has less snow, but higher mountains and better rock exposure (Fig. 2).

The Russian and Mongolian Altai contain numerous peaks over 4000 m and permanent snow and glaciers starting at approximately 3600 m. The Altai widens to the NW and joins with the Sayan Mountains in Russia, whereas at its SE end it narrows and is topographically joined to the Gobi Altai (Fig. 1). The Altai is bordered on the east by the wide Valley of Lakes, which receives sediment transported by rivers and wind from the Altai to the west. There is no evidence that the Valley of Lakes is downdropped (Cenozoic normal faults have not been found and people have looked for them), rather the Altai is simply uplifted relative to the Valley of Lakes. Likewise, the Junggar Basin borders the Altai to the west on the Chinese side, but has not been downdropped, rather the Altai has been uplifted relative to it. The Mongolian Altai is dominated by discrete block uplifts or topographic culminations which are generally asymmetric and elongate to the NW.

The Mongolian Altai is tectonically active with well-documented historic earthquakes and associated ground rupturing (see review in Baljinnyam *et al.* 1993; Bayasgalan *et al.* 1999). The major faults in the region are NW-trending throughout the range and accommodate dextral strike-slip, oblique-slip, and thrust motions. Other indicators of modern fault activity include sharply defined mountain fronts with low sinuosity, active alluvial fan deposition along steep range fronts, displaced Quaternary alluvium and glacial deposits, offset streams, asymmetric drainage patterns suggesting block tilting, steep canyons with active river incision, and preserved peneplained summits indicating recent uplift of mountain blocks. Satellite images of the region show prominent NW-striking faults which variably link and diverge and in some cases can be traced for hundreds of kilometres (Figs 3, 4). GPS studies of active deformation in the Altai region indicate that crustal motion is currently northward directed at approximately 1 cm a^{-1} relative to a fixed Siberia (J. Deverchere, E. Calais, pers. comm. 2001). The maximum horizontal stress in the

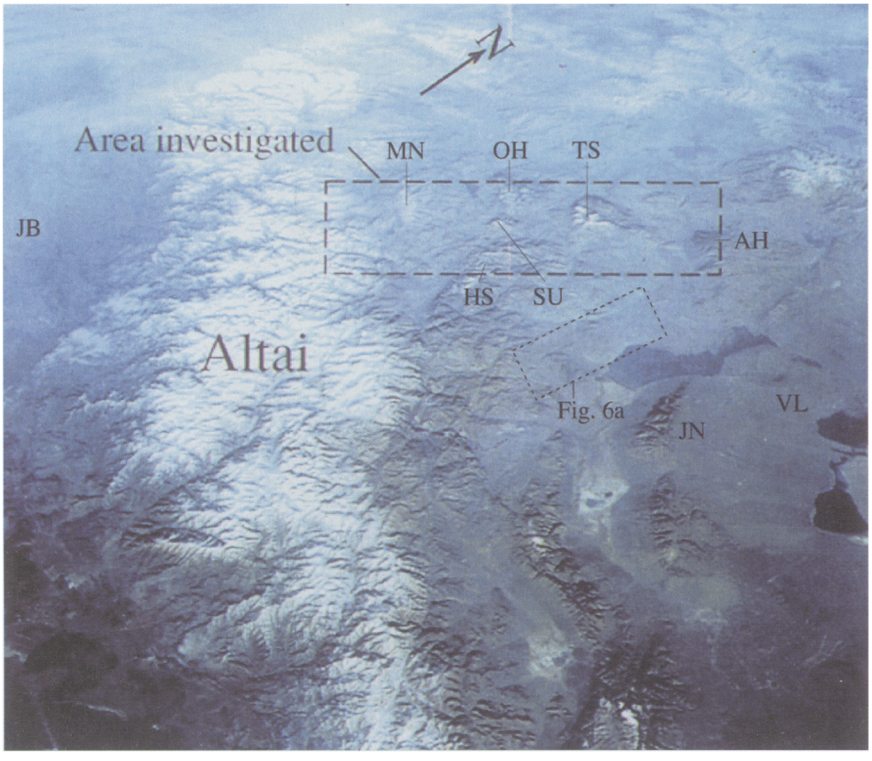

Fig. 2. Oblique shuttle photograph #STS74–713–005 looking NW of Chinese and Mongolian Altai region. Area investigated and individual block uplifts described in text are indicated. JB: Junggar Basin; VL: Valley of Lakes; MN: Mengildyk Nuruu; OH: Omno Hayrhan Uula; TS: Tsambagarav Massif; AH: Altun Huhey Uul; HS: Hoh Serhiyn Nuruu; SU: Sutai Uul; JN: Jargalant Nuruu. Location of Figure 6a also shown.

region is approximately NE–SW based on earthquake data (Zoback 1992).

Regional geology

Basement rocks throughout the Mongolian Altai are generally greenschist grade metasedimentary and metavolcanic rocks dated as Lower Palaeozoic (Fig. 5; Zaitsev 1978). Precambrian rocks have not been identified in the region of this study. Precambrian continental slivers are reported from the Chinese Altai (Qu & Chong 1991; Qu & Zhang 1994) and southernmost Mongolian Altai (Mongolian National Atlas 1990), but there are few reliable published ages. The Lower Palaeozoic basement rocks comprise monotonous greenschists, phyllites, and slates which generally dip ENE and strike NW; this prevailing basement grain dominates the structure of the Altai. These rocks are metapelitic and metabasic and are internally folded and foliated displaying at least two phases of NE–SW-directed contractional ductile deformation. Cutting the basement are numerous granitoids of early–late Palaeozoic age. Unconformably overlying the metamorphic basement are Devonian sedimentary rocks dominated by red continental clastic sediments and shallow marine turbidites. Interpreting the tectonic setting of the basement rocks is controversial; however, the great thicknesses of metasedimentary and metavolcanic rocks suggest that they were deposited in a subduction complex or arc-proximal setting and were contractionally deformed during the Cambrian–Silurian (Sengör *et al.* 1993; Sengör & Natal'in 1996).

Mesozoic rocks are rare in the Altai, but Mesozoic coarse clastic sediments including coal-bearing conglomerates are found in flanking basins to the east suggesting an eroding source area existed in the Altai region during Jurassic–Cretaceous time (Sjostrom 1997; Howard *et al.* in press). No evidence for Mesozoic contractional deformation has yet been found in the Altai, unlike the Tien Shan to the south (Hendrix *et al.* 1992). Jurassic–Cretaceous extensional tectonism was widespread in the Gobi Altai region and may have affected the Altai region also (Traynor & Sladen 1995; Webb *et al.* 1999).

Cenozoic rocks consist of continental clastic

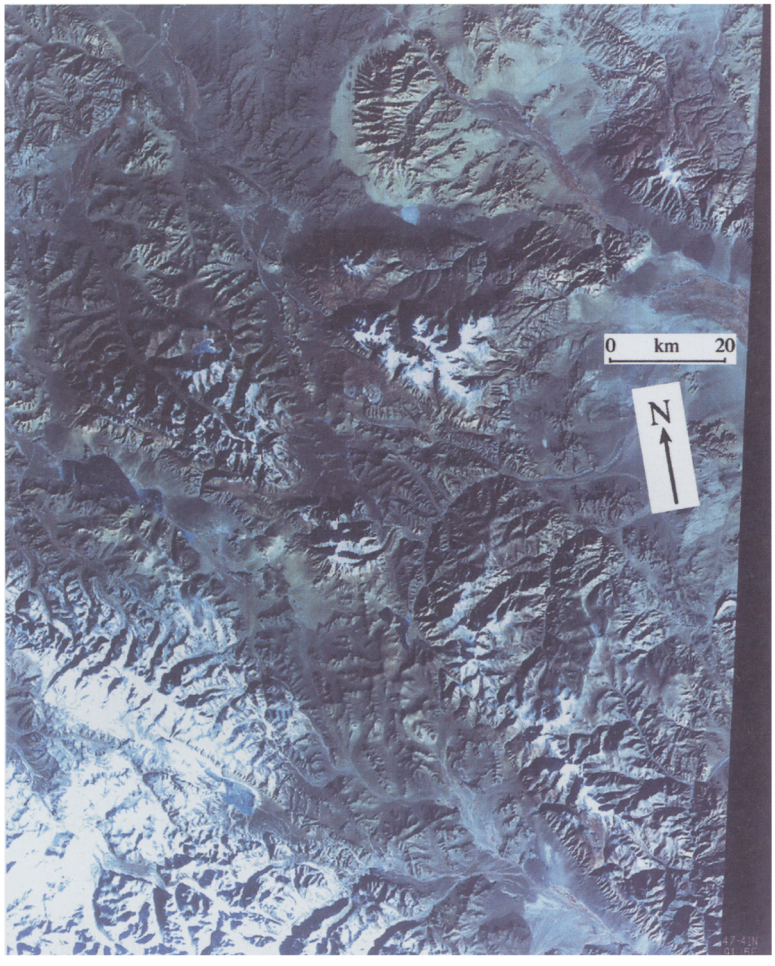

Fig. 3. Landsat MSS image of part of Mongolian Altai investigated in this study. Location of image shown in Figure 1. Notice discrete mountain blocks and numerous sharply defined NW-trending faults. Image interpretation is shown in Figure 4.

sequences that fill basins in the adjacent Valley of Lakes to the east of the Altai, and locally derived alluvial, fluvial, and glacial sequences that fill small intramontane basins within the Altai. The sedimentary record indicates a rapid increase in erosion and coarse locally derived clastic sedimentation beginning in the Miocene and continuing to the present (Devyatkin 1974). This record is the best indicator of the timing of Cenozoic reactivation and uplift of the Altai in Mongolia.

Field results

The study area can be subdivided into seven discrete structural blocks or domains which are characterized by a major range bounding fault and adjacent block uplift (Figs 3, 4). Each domain will be described proceeding from NE to SW.

Altun Huhey range

Altun Huhey Uul is a major block uplift on the eastern edge of the Altai bordering the Valley of Lakes to the east (Fig. 2). The range is topographically asymmetric with a sharply defined steep SW mountain front in contrast to a gently sloping E and NE slope (Figs 3 & 6). The SW mountain front is marked by fresh alluvial fans, steep relief, and short steep canyons cutting into the range. A degraded fault scarp cuts one of the fans (Fig. 7a, b) suggesting Quaternary activity. This scarp has up to 18 m of measured vertical displacement sug-

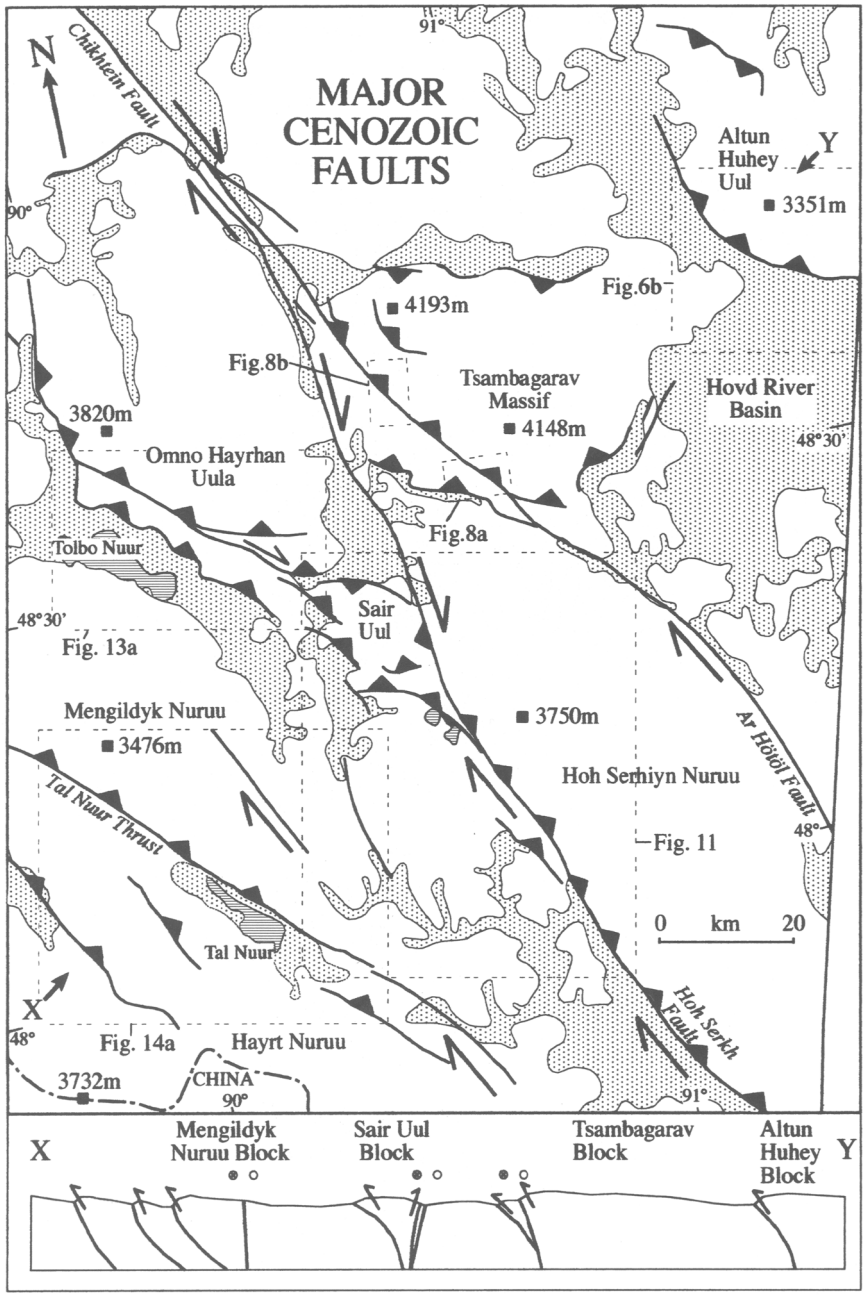

Fig. 4. Interpretation of Figure 3 showing major Cenozoic faults and sedimentary basins, northwestern Mongolian Altai. Locations of subsequent figures shown. Cross section (scaled down) shows interpreted block geometry.

gesting it records multiple earthquake events. Sense of movement is NE-side-up.

At the mountain front itself, a SW-directed thrust fault is well exposed in a dry stream canyon (Fig. 7c) at 48°43.08′N, 91°32.49′E. This fault places biotite quartzofeldspathic gneisses over quartzofeldspathic mylonitic gneisses. The fault zone is brecciated over a thickness of at least 50 m and contains many slickensided gouge zones that define discrete plane of brittle shearing. The major

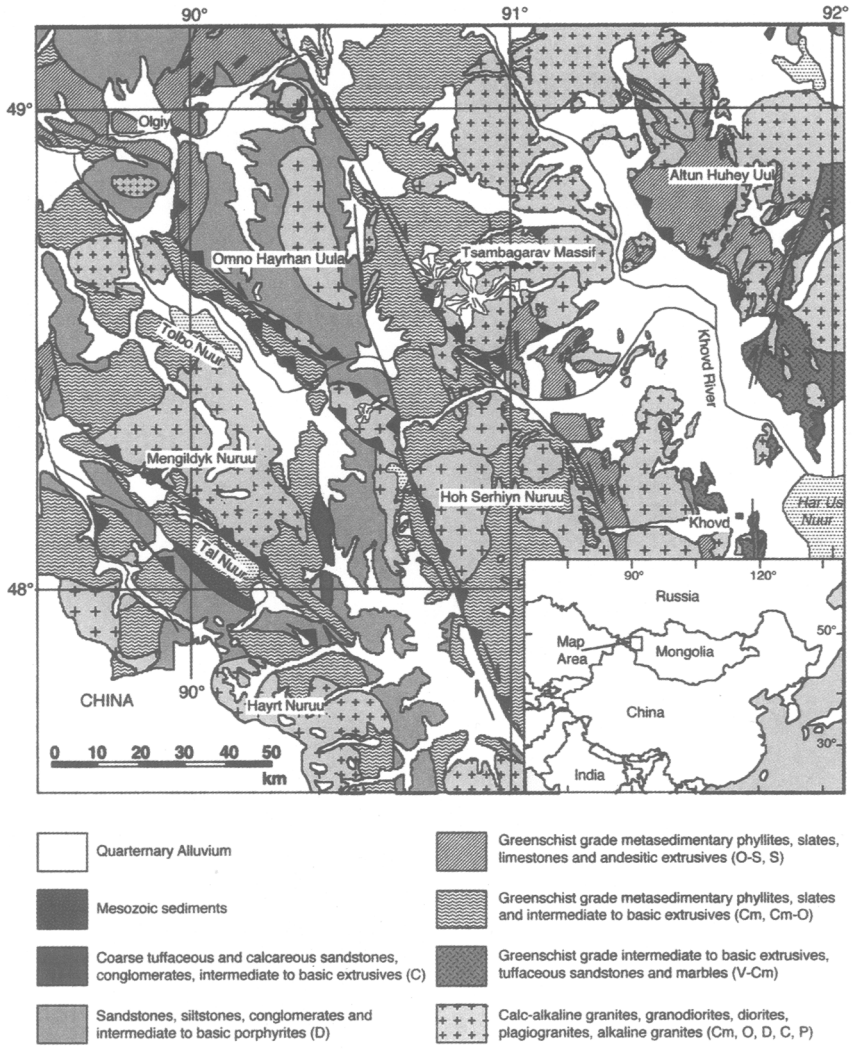

Fig. 5. General lithological map of the western Mongolian Altai. Map area is similar to region shown in Figures 3 and 4. Basement rocks are dominantly Lower Palaeozoic metasedimentary and metavolcanic rocks intruded by younger Palaeozoic granitoids. Map adapted from Zaitsev (1978). V: Vendian; Cm: Cambrian; O: Ordovician; S: Silurian; D: Devonian; P; Permian.

fault plane strikes 321, dips 22°NE, and contains slickensides plunging 18°, 032, indicating a dextral component to the thrusting. The kinematics are clear due to the presence of 0.5–1.0 m asymmetric folds, dragged layers, and thrust repeated layers. The brittle thrust fabric is locally parallel to the gneissic fabric suggesting possible reactivation of the basement anisotropy. Elsewhere, the fault truncates the older basement structures.

These two fault zones are responsible for Cenozoic uplift and NE tilting of the Altun Huhey range. Reconnaissance work elsewhere in the range and examination of satellite imagery (Fig. 3) and aerial photographs failed to reveal other major Cenozoic thrust faults. The frontal thrusts lie near the northern end of the Hovd dextral strike-slip fault (Figs 2, 6a) which passes into and possibly through the range at its eastern end (Fig. 6a, b). The frontal thrust faults can be traced towards the SE, where they probably link with the Hovd Fault, although the fault junction is not exposed (Fig. 6b).

Tsambagarav Massif

The Tsambagarav Massif is a topographic and structural culmination along the trend of the

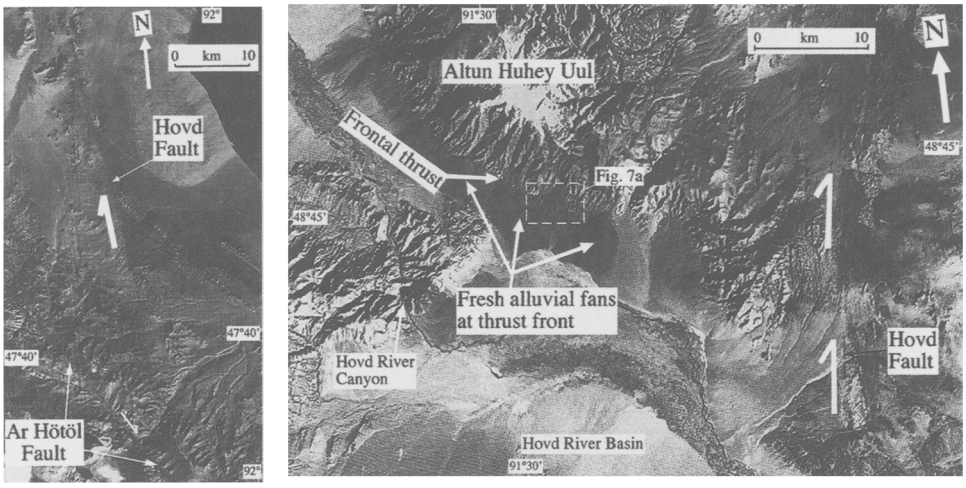

Fig. 6. (**a**) Kosmos image of Hovd dextral strike-slip fault. See Figure 2 for location of image. Note drag of sedimentary layers on fault's east side indicating dextral sense of motion. Fault disappears without surface rupture under Hovd River Basin to north, but appears to re-emerge along strike in eastern Altun Huhey Uul (Fig. 6b). (**b**) Kosmos image of Altun Huhey (also see Landsat view, Fig. 3) showing sharply defined SW mountain front, fresh alluvial fans, Hovd River canyon and suggested along-strike continuation of Hovd Fault. Altun Huhey Uul frontal thrust is believed to accommodate some of Hovd Fault's dextral motion. Location of Figure 7a shown.

regionally extensive Ar Hötöl dextral strike-slip fault system (Figs 3, 4). The range is topographically asymmetric with a steep SW mountain front and a regionally peneplained summit that is ice-covered and gently NE tilted (Fig. 9a). The range has a peculiar triangular shape with high relief on all sides except around the NE corner.

The range is dominantly composed of intrusive rocks and paragneissic greenschist–amphibolite grade basement rocks. The intrusive rocks range from gabbro to granite in composition.

The SW front of the range is marked by a major active fault system that is clearly visible on satellite and aerial photographs (Figs 3, 8). This fault is part of the regional Ar Hötöl system (cf. Baljinnyam *et al.* 1993) and in this study is referred to as the Main Tsambagarav Dextral Reverse Fault. This fault system was examined in detail in various places along the range front where evidence for recent activity includes fresh scarps (Fig. 9b, c), en echelon tension gashes (Figs 8a, 9e), a sag pond (Figs 8a & 9d), and offset morainal deposits (Fig. 8a). The offset morainal deposits and orientation of en echelon fissures indicate dextral displacement (Fig. 8a). The main frontal fault scarp is remarkably linear on aerial photographs and can be seen to dip steeply NE where it cuts across valleys (Fig. 8b) The scarp vertically offsets recent alluvial deposits (Fig. 9c) by up to 6–7 m, indicating NE-side-up reverse displacement in addition to the dextral history. The scarp is generally a compound feature with preserved vertical separations as high as 32 m due to multiple surface rupture events.

The Main Tsambagarav Dextral Reverse Fault is beautifully exposed where a major canyon cuts through it at the NW end of the Tsambagarav Massif at 48°38.488′, 90°43.360′, 2880 m elevation (Figs 9f–h). At this location, the fault zone is up to 300 m wide and contains many semi-parallel fracture surfaces striking 320 ± 20° and dipping vertically to steeply NE with widespread brecciation between fracture surfaces. Much of the zone is iron-stained and clay-altered. The centre of the fault zone is an impressive 8–10 m wide zone of soft greenish gouge (Fig. 9h). This is a rare outcrop of the core zone of a regional-scale strike-slip fault. The gouge is literally oozing out of the cliff and spreading downward as soft mudflows and individual debris flows (Fig. 9h).

At this canyon location, sense of movement on the fault is interpreted to be dextral reverse for the following reasons: the stream is diverted NW as it crosses the fault (Fig. 9f), fractures within the fault zone and the fault itself clearly dip steeply NE (Figs 8b, 9g), and the local relief across the fault indicates NE-side-up displacements. Slickensides are rare within the fault zone and where measured trend between 312 and 047°, which is consistent with both dextral and thrust displacements. Upper-plate rocks consist of mylonitized biotite–muscovite–quartzofeldspathic gneiss. The main mylonitic fabric strikes, 327 and dips 78°NE with

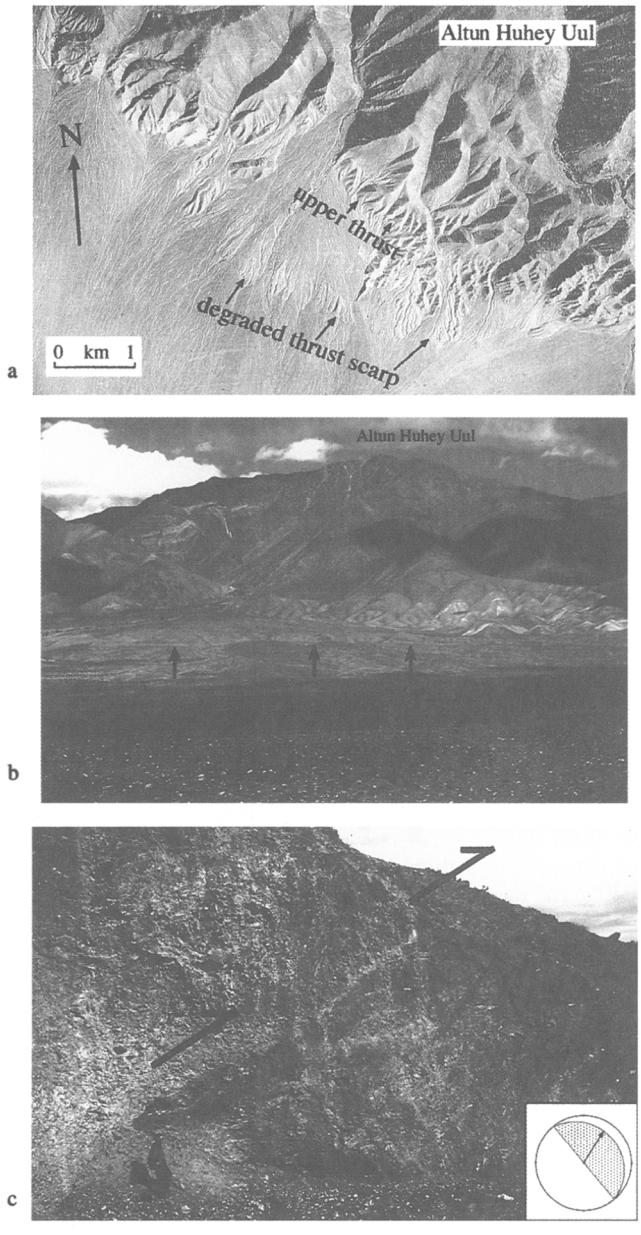

Fig. 7. (**a**) Aerial photo of SW front of Altun Huhey Uul showing degraded thrust scarp which cuts Quaternary alluvial fan (also see Fig. 7b) and location of frontal thrust shown in Fig. 6c. (**b**) View NE of steep relief along SW front of Altun Huhey Uul and faulted alluvial fan (arrows). (**c**) View ESE of frontal thrust ('upper thrust' in Fig. 7a) which bounds SW front of Altun Huhey Uul (48°43.08′, 91°32.49′). Inset shows equal area, lower hemisphere stereographic projection of brittle fault plane and trend and plunge of slickenlines.

a well-developed subhorizontal quartz and mica lineation. Good S-C fabrics and asymmetric quartz vein boudins indicate left-lateral shear sense. This fabric is approximately parallel to the brittle fractures and main fault trace of the Main Tsambagarav Dextral Reverse Fault at the mountain front suggesting that it has reactivated the older ductile mylonitic fabric.

SE of the Main Tsambagarav Dextral Reverse Fault at a topographically lower level, another

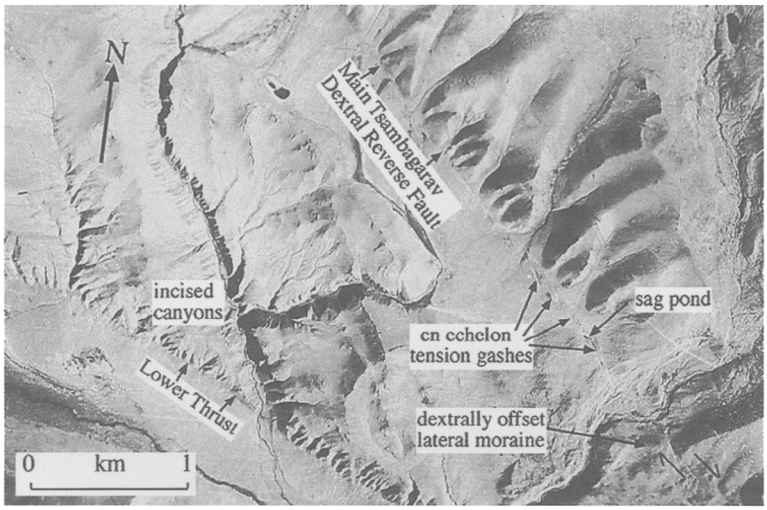

a

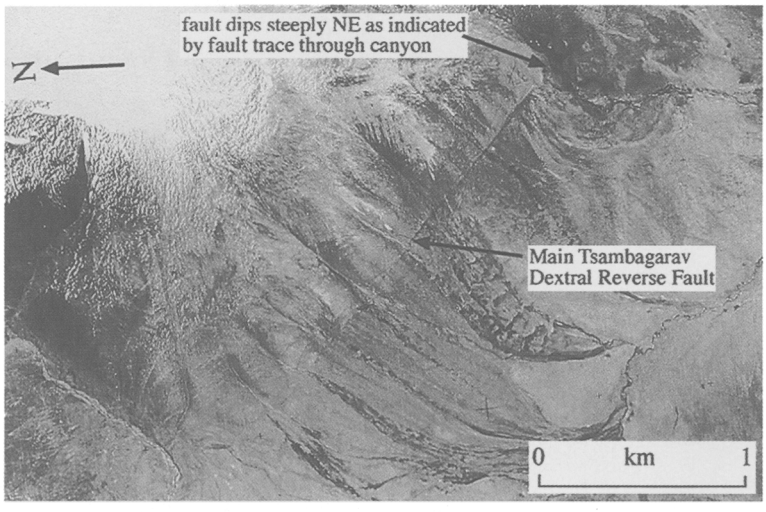

b

Fig. 8. (**a**) Aerial photo of active faults which bound SW front of Tsambagarav Massif. Note dextrally offset glacial deposits (arrows) and en echelon tension gashes suggesting dextral offset (48°32.612′, 90°50.314′). Location of photo shown in Figure 4. (**b**) Aerial photo of sharply defined Main Tsambagarav Dextral Reverse Fault, NW end of SW mountain front (48°38.295′N, 90°43.735′E).

major fault was identified which is visible on satellite and aerial photos as a major step in the topography ('Lower Thrust' on Fig. 8a). This fault also appears to have an important thrust history which has uplifted biotite–muscovite–garnet schists in its upper plate. Steeply incised canyons cut the upper plate suggesting that streams have been forced to incise downwards as the block was being thrusted upwards (Fig. 8a). This fault also cuts alluvial deposits at the mountain front suggesting recent activity (Fig. 10a). The scarp has up to 17 m of vertical displacement measured across it presumably due to multiple surface rupture events.

The schists at the mountain front are ultramylonitic with a strongly developed quartz stretching lineation (Fig. 10b). The schists strike 308 and dip 20°NE with lineations plunging 14°, 016. Away from the front, the schists are not mylonitic. Brittle gouge zones that are fabric parallel are abundant within the mylonite directly at the front. Thus the modern fault has reactivated older ductile fabrics.

From a regional perspective, the Tsambagarav

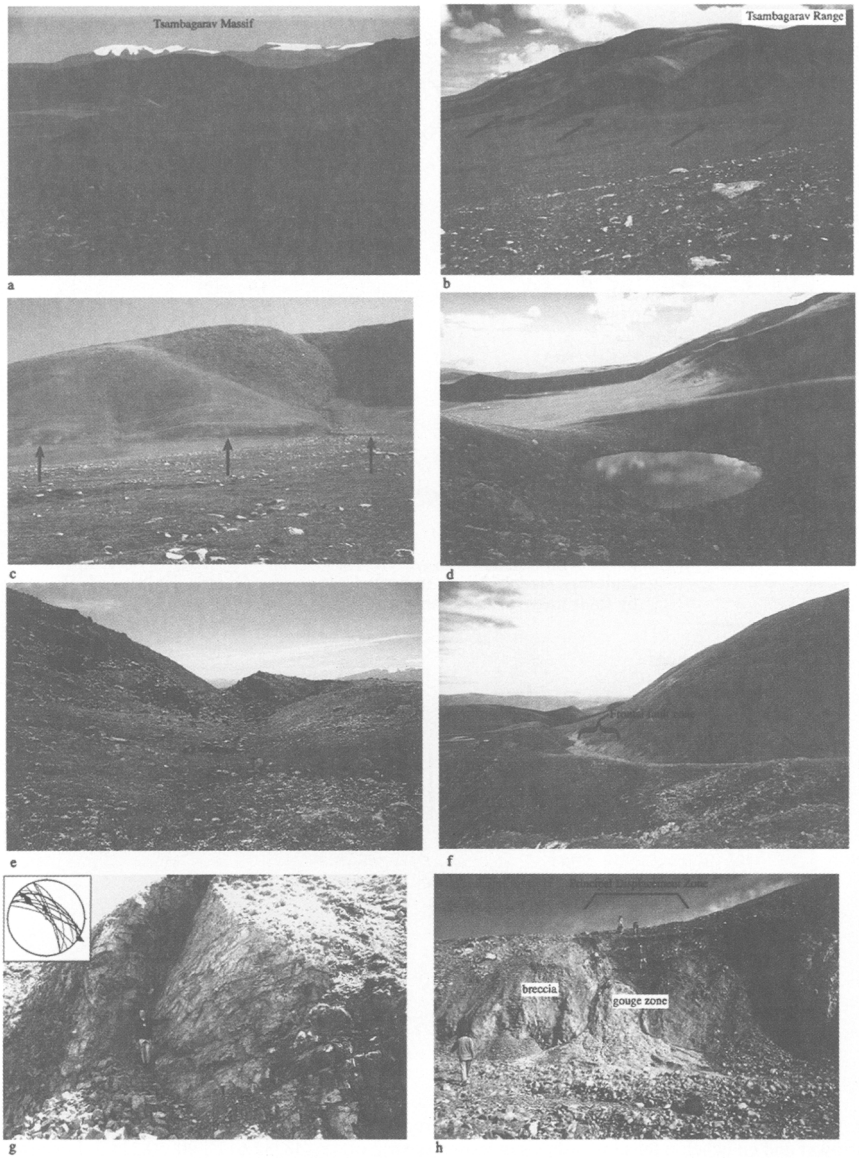

Fig. 9. (**a**) Distant view NE of Tsambagarav Massif. Flat summits preserve Cretaceous–Palaeogene peneplain now capped by glaciers. (**b**) View NE of Main Tsambagarav Dextral Reverse Fault along SW front of Tsambagarav Massif. Scarp has linear Holocene rupture trace and is locally marked by springs and green grass (48°32.612′, 90°50.314′). (**c**) Surface rupture of Main Tsambagarav Dextral Reverse Fault along SW mountain front, Tsambagarav Massif (48°34.323′, 90°48.166′). (**d**) Small sag pond along trace of Main Tsambagarav Dextral Reverse Fault, SW front of Tsambagarav Massif (see Fig. 8a for location). (**e**) Open tension cracks along trace of Main Tsambagarav Dextral Reverse Fault at 48°38.295′N, 90°43.735′E. Cracks are left stepping and en echelon suggesting dextral strike-slip movement. Person in centre middle distance for scale. (**f**) View NW of unnamed canyon, NW end of SW front of Tsambagarav Massif (48°38.295′N, 90°43.735′E). Main Tsambagarav Dextral Reverse Fault is nicely exposed along canyon walls (Fig. 9g, h). Note steep mountain front and deflection of drainage to NW at canyon outlet where river crosses fault. (**g**) Photo looking SE of brittle fault plane within Main Tsambagarav Dextral Reverse Fault at canyon outlet (location shown in Fig. 9f). Inset shows equal area, lower hemisphere stereographic projection of brittle fault planes within fault zone. Arrows indicate trend and plunge of fault plane slickenlines. (**h**) Photo looking SE of impressive 8 m wide gouge zone of Main Tsambagarav Dextral Reverse Fault exposed in canyon walls. This is interpreted as the core displacement zone for the Main Tsambagarav Dextral Reverse Fault (48°38.488′, 90°43.360′).

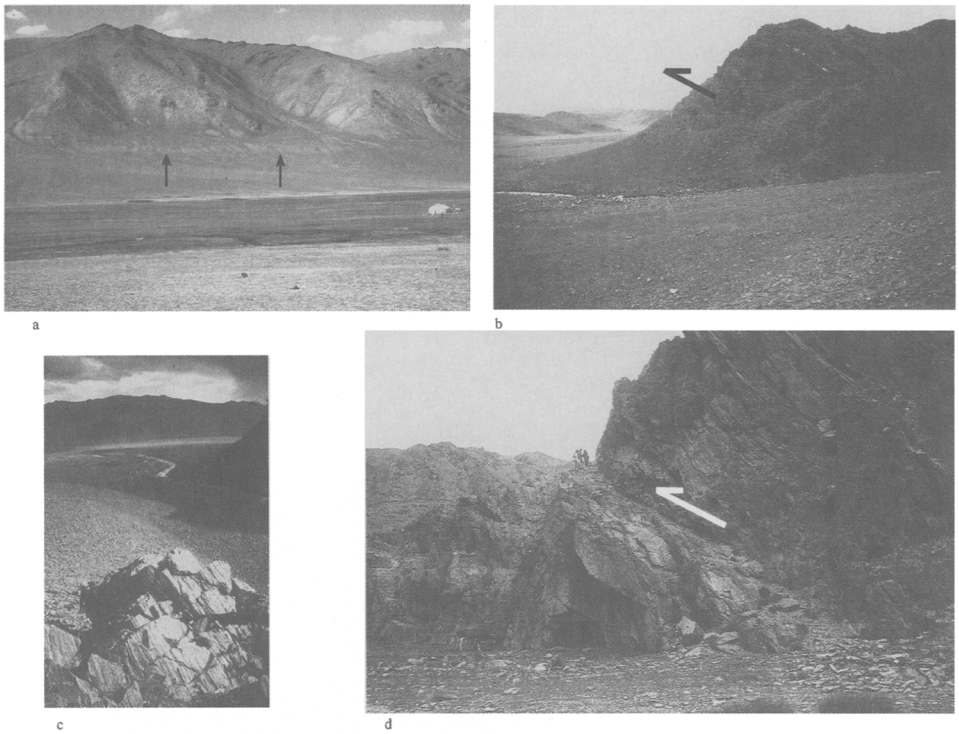

Fig. 10. (**a**) View NE of Holocene surface rupture of lower Tsambagarav thrust fault (48°32.703′, 90°43.618′). See Figure 8a for aerial photo perspective. (**b**) View NW of lower Tsambagarav thrust front where ductile mylonitic fabrics are reactivated by brittle thrust faulting (48°34.323′, 90°48.166′). (**c**) View SW of mylonitic quartzites and mica schists which have been brittlely reactivated by lower Tsambagarav thrust (same location as Fig. 10b). (**d**) Brittle SW-directed thrust (348°, 28NE) cutting lower greenschist grade phyllites approximately 10 km SW of lower Tsambagarav thrust along Hachat Gol Valley (48°23.965, 90°49.905′). For location see Figures 4, 11.

range forms an uplifted triangular block at a gentle restraining bend along the Ar Hötöl/Chikhtein Fault (Figs 3, 4). Active transpressional deformation is expressed by reverse motion and dextral strike-slip displacements that clearly offset Quaternary sedimentary deposits. Pre-existing ductile mylonite zones helped control the location of the Cenozoic faults which clearly reactivate older structural anisotropy along some sections of the range front. SW of the Tsambagarav range along the Hachat Gol canyon (Fig. 11), we observed several other NE-striking, SW-directed thrust faults which brittlely cut the basement phyllites and slates (Fig. 10d). These faults are not expressed on satellite imagery and their age is uncertain.

Sair Uul

Sair Uul is a major structural and topographic culmination that has formed between divergent splays of the regionally extensive Hoh Serkh dextral strike-slip fault (Figs 3, 4, 11). The eastern side of the range is bounded by a linear fault that appears on satellite imagery to link northwards with the Chikhtein Fault (Fig. 3). This fault cuts through glacial deposits suggesting Quaternary movement and is interpreted to have a reverse component of motion responsible for uplift of the eastern side of Sair Uul. The western side of Sair Uul is bounded by several thrust faults which have also uplifted the range (Fig. 11). The range is therefore interpreted to be a structural pop-up with an asymmetric flower structure geometry. The range was not studied in detail; however, fault scarps cutting alluvium were observed from a distance along the range's NW mountain front suggesting Quaternary movement. Major glacial valleys and streams within the range drain eastwards suggesting bulk eastward tilting due to thrusting on the west side (Fig. 3).

Hoh Serhiyn Nuruu

This range is bounded on the NE by the dextral Ar Hötöl Fault and on the SW by the Hoh Serkh Fault (Figs 3, 4). The Hoh Serkh Fault was previously referred to as the Tolbo Nuur Fault (Baljinnyam

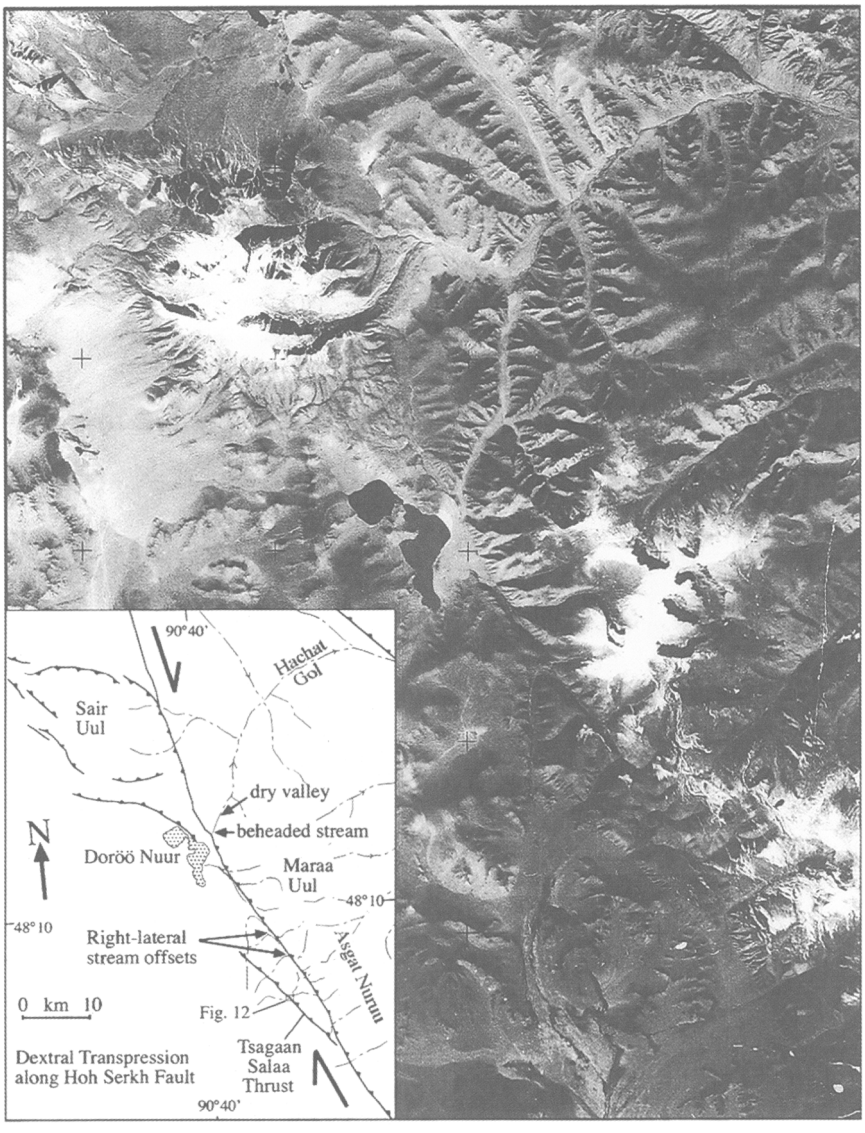

Fig. 11. Kosmos image of Sair Uul and Asgat Nuruu region and active deformation along length of Hoh Serkh Fault. See Figure 4 for exact location of image. Inset map shows interpretation of major Cenozoic faults and important geomorphological features. Location of Figure 12 shown.

et al. 1993) and Hovd-Olgiy Fault (Tapponnier & Molnar 1979); however, the fault cannot be traced continuously to Tolbo Nuur (Figs 3, 4), nor does it pass close to the towns of Hovd or Olgiy (Figs 4, 5) and so these names are considered misleading. The Hoh Serkh Fault is a regionally important dextral strike-slip fault with a reverse component of motion. The dextral component is clearly observed on satellite imagery near Maraa Uul where six large streams are consistently offset in a dextral sense (Figs 3, 11, Tapponnier & Molnar 1979). The reverse component is inferred by the steep relief at the mountain front and the asymmetric tilt of the Hoh Serhiyn range which has its drainage divide close to the SW mountain front (Fig. 3). The Hoh Serkh Fault forms an impressive linear valley below Maraa Uul and Asgat Nuruu (Fig. 11); however, along this trace, no fresh scarps were found.

Where the fault enters the Doroo Nuur Basin (Fig. 11), there is a very degraded trace of a surface rupture that is only locally discernible.

Below Asgat Nuruu and SW of the Hoh Serkh Fault, a separate thrust fault was identified which is responsible for uplifting the small range where the prominent dextrally offset streams are found (Fig. 11). We name this fault the Tsagaan Salaa Fault after the canyon where it is best exposed. This fault is similar to the lower thrust at the Tsambagarav Massif in that it: (1) appears to splay off of a major dextral strike-slip fault (the Hoh Serkh Fault) at its SE end, but dies out to the NW, (2) uplifts metasedimentary schists in its hanging wall, and (3) forms a prominent step in the topography. It also forms a major scarp visible from a distance (Fig. 12a; GPS: 48°03.239′N, 90°45.994′E) and excavations along the scarp indicate that it contains a well-developed brittle fault fabric striking 334, 36°NE (Fig. 12b, c). Slickenlines plunge moderately NE, but were poorly preserved or generally absent. The fabric in the basement schists is SW dipping at the mountain front and therefore the NE-dipping brittle thrust fabric cuts across the basement structural anisotropy instead of reactivating it.

Above the fault, the Tsagaan Salaa canyon is deeply incised and there are small waterfalls at the frontal scarp (Fig. 12b) suggesting recent uplift. Upstream, there is a prominent terrace perched 2–4 m above the modern stream suggesting forced river incision due to thrusting at the mountain front.

Doroo Nuur is a lake that fills a small basin along the northern extent of the Hoh Serkh Fault where the fault divides into two branches that bound the Sair Uul Block (Fig. 11). The lake appears to have once been linked to the SW branch of the Hachat Gol (Fig. 11), which is a major valley with a dry stream bed. The depth of valley incision and size of the stream bed suggest that the valley once contained a major stream. The valley is unusual in the region because other similar sized valleys contain perennial streams.

There is only a small topographic rise between the Doroo Nuur and the SW branch of the Hachat

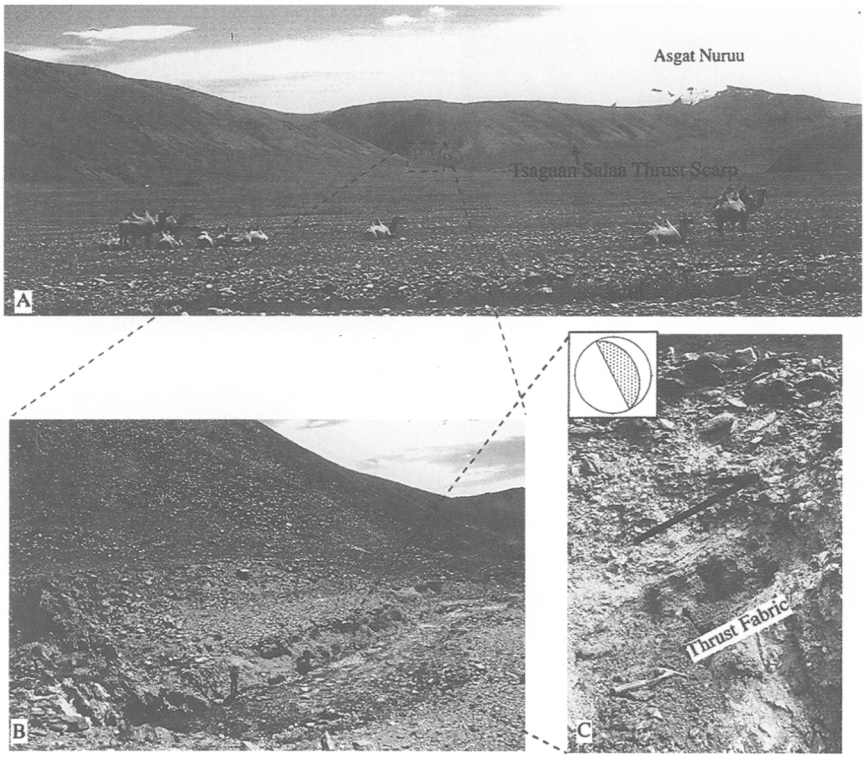

Fig. 12. (**a**) Distant view eastwards of Tsagaan Salaa thrust fault, Asgat Nuruu. See Figure 11 for exact location. Boxed area is shown in Figure 12b. (**b**) View SE at thrust front showing stream cut where fault is exposed. Note waterfall at thrust front and incised terrace. Boxed area is shown in Figure 12c. (**c**) View SE of boxed area shown in Figure 12b where brittle thrust fabrics are exposed within Tsagaan Salaa thrust zone, Asgat Nuruu (48°03.239′, 90°45.994′). Main fault strikes 334° and dips 36°NE as shown by equal area, lower hemisphere stereographic projection (inset).

Gol. This topographic boundary is fronted by the Hoh Serkh fault zone which further south clearly has a reverse component of motion which has uplifted the Hoh Serhiyn range and tilted it eastwards. It is suggested that the continued activity of this fault has led to uplift on the east side of the fault which has dammed and beheaded the SW branch of the Hachat Gol and removed much of its catchment area. Doroo Nuur now receives the runoff that previously flowed down the SW Hachat Gol valley (Fig. 11).

The tectonic geomorphology along the length of the Hoh Serkh Fault indicates that the kinematics of active deformation change along strike. When viewed from the SE, the east side of the Hoh Serkh Fault is uplifted as far north as Doroo Nuur. Further north, the west side of the fault is uplifted where it bounds Sair Uul's steep eastern front. This suggests that the fault segment with the least amount of reverse displacement is adjacent to Doroo Nuur where the fault bends to a more northerly trend (Fig. 11). Oblique kink bands with combined normal and dextral senses of motion were observed in phyllites directly SE of Doroo Nuur along the trace of the Hoh Serkh Fault suggesting that, if they are Cenozoic structures, a possible transtensional component of motion may have also contributed to the development of the Doroo Nuur Basin.

Omno Hayrhan Uula

This range forms a major block uplift NW of Sair Uul and has large actively forming alluvial fans along its SW margin (Fig. 3). These fans are shed into an intermontane basin where they bound Tolbo Nuur (Fig. 13a). The SW front of Omno Hayrhan Uula is a major thrust zone that locally cuts Quaternary alluvium indicating recent activity (Fig. 13b, c). Degraded scarps up to 10 m high occur along the front. At the SW end of the range, several step-like scarps are present which represent thrust faults that have elevated the region where Sair Uul and Omno Hayrhan Uula join (Figs 3, 13a).

The SW Omno Hayrhan Uula mountain front is particularly interesting at the entrance to the Bort

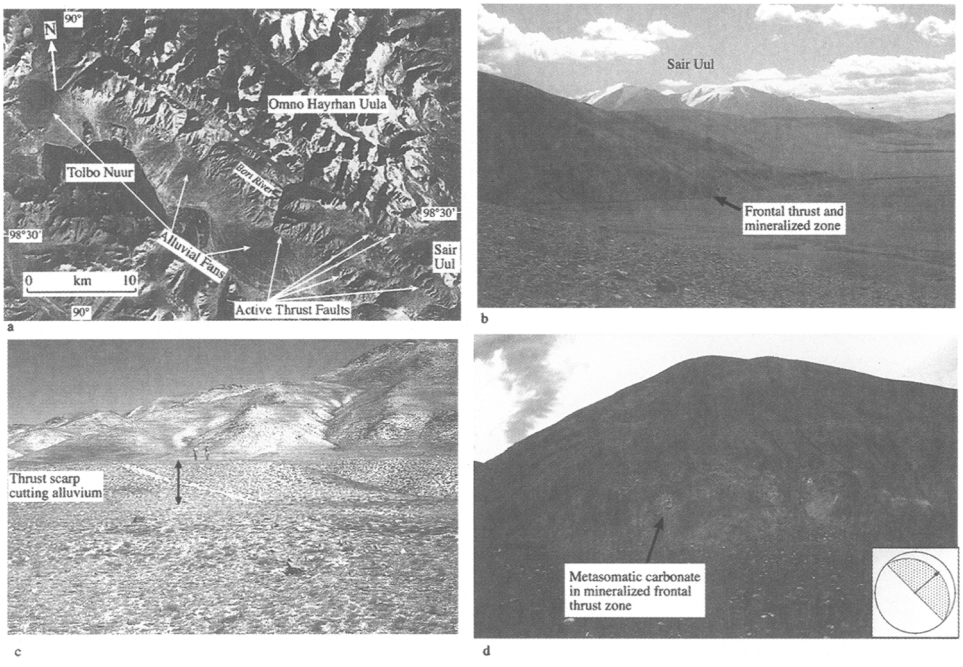

Fig. 13. (**a**) Kosmos image of Tolbo Nuur and Omno Hayrhan Uula region, Mongolian Altai. Omno Hayrhan Uula is bound by SW-directed thrust faults on its SW side. Fresh alluvial fans along the mountain front help define the limits of Tolbo Nuur. Note dextral offsets on Bort River canyon and the major canyon NW of Bort River. For location of image see Figure 4. (**b**) View SE of SW frontal thrust zone at entrance to Bort River canyon, Omno Hayrhan Uula. Sair Uul pop-up in distance. Fault is a Palaeozoic shear zone containing Fe–Ti mineralization which has been reactivated by brittle Cenozoic thrusting. (**c**) View NNE of surface rupture of thrust fault, SW front of Omno Hayrhan Uula (48°02.899′, 90°17.054′). Scarp has approximately 5 m of vertical offset. (**d**) View NE of brittle frontal thrust zone cutting Palaeozoic mineral deposit, entrance to Bort River canyon, SW front of Omno Hayrhan Uula (48°29.947′, 90°15.252′). Inset shows equal area, lower hemisphere stereographic projection of fault plane.

River canyon (48°29.947′, 90°15.252′, 2280 m). In the front range, the Bort River cuts through a sequence of lower greenschist grade metamorphosed volcaniclastic sediments, and volcanic breccias. However, at the mountain front, this sequence forms the upper plate of a brittle thrust zone which contains visually impressive Fe–Ti mineralization, serpentinite alteration, and metasomatic carbonate development (Fig. 13d). The mineral deposit only occurs within the thrust zone which strikes 315°, dips 24NE, and contains slickenlines plunging 24, 050°. This mineralization is believed to be hydrothermal in origin, perhaps related to metamorphism in a marine volcanic and volcaniclastic sequence. Thus the mineralization is believed to be Palaeozoic in age when Altai regional metamorphism last occurred. Therefore, modern Cenozoic thrusting at the mountain front has reactivated an older mineralized Palaeozoic fault zone.

Another major Cenozoic fault zone forms a prominent linear valley within Omno Hayrhan Uula approximately 5 km up the Bort River canyon from the mountain front (Figs 3, 13a). This fault zone dextrally offsets two major river systems which drain the range (Fig. 13a) and the fault is well exposed along the cliffs of the Bort River canyon. At the fault zone (48°32.117′N, 90°18.233′E), brittle thrusts diverge from its core in flower-like geometry over a width of approximately 80 m. The main fault strand is a vertical, 325°-striking, 2 m thick cemented breccia which cuts through sheared phyllites composed of metasediments and metavolcaniclastic rocks. Rocks to the SW and NE are increasingly unmetamorphosed in appearance within only a few hundred metres suggesting that the fault zone is a local peak metamorphic zone perhaps due to concentrated fluid flow along it. Some of the fault rocks are best described as fault schists and contain strongly developed S-C fabrics indicating SW-directed thrusting within the SW part of the fault zone.

Investigations in the remainder of Omno Hayrhan Uula were not carried out; however, examination of satellite imagery suggests that only the S, SW, and W sides of the range have experienced Cenozoic fault activity. Further to the NW, Baljinnyam *et al.* (1993) reported surface ruptures along the mountain front directly NE of Tolbo Nuur. Satellite imagery indicates that the range's drainage systems are markedly asymmetric with most rivers running E or NE away from the active W and SW

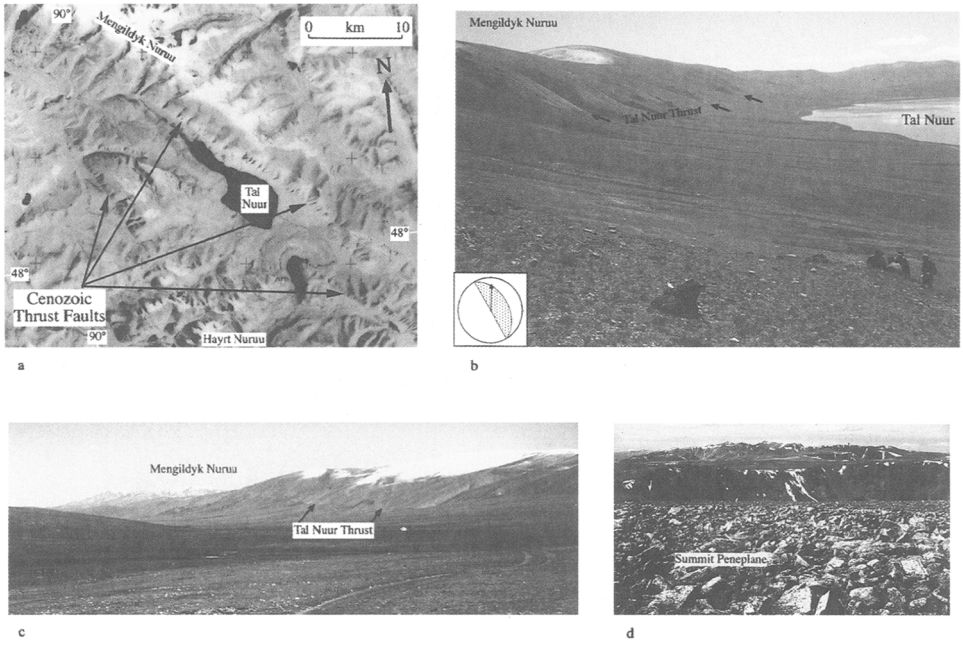

Fig. 14. (**a**) Kosmos image of Tal Nuur region, Mongolian Altai. See Figure 4 for location. Tal Nuur fills depression bounded by Mengildyk Nuruu to NE which is uplifted along the SW-directed Tal Nuur thrust fault. (**b**) View SE of Tal Nuur thrust which is marked by break in slope along SW front of Mengildyk Nuruu (48°02.899′, 90°13.735′). Inset shows equal area, lower hemisphere stereographic projection of brittle fault plane. (**c**) View north towards Mengildyk Nuruu and clearly defined Tal Nuur thrust. (**d**) View NW of summit ridge of Mengildyk Nuruu showing preserved Cretaceous–Palaeogene peneplain at 3450 m elevation (48°11.102′. 90°08.007′).

mountain fronts. Thus the Omno Hayrhan range is regarded as an asymmetrically NE-tilted Cenozoic block uplift.

Mengildyk Nuruu

Mengildyk Nuruu is a flat-summitted, NW-trending range which is bounded on its SW side by the Tal Nuur Basin (Figs 3, 14). The SW range front is abrupt and marked by the Tal Nuur thrust, a major Cenozoic thrust fault which is largely responsible for uplift of the range (Fig. 14a–c). Directly east of Tal Nuur, this fault places granite and green metasedimentary phyllites over tilted, and locally overturned and folded, red Devonian clastic sediments. The fault forms a scarp that is locally up to 40 m high. The granite at the scarp itself is pervasively fractured with a strong brittle fabric striking 330°, dipping 42NE, and containing slickenlines plunging 24, 002°. At the SE end of Mengildyk Nuruu, the Tal Nuur thrust appears to change its polarity because the SW side of the fault is uplifted along two en echelon segments (Fig. 3).

Hayrt Nuruu and the Chinese Altai

Our investigations in Hayrt Nuruu and the Chinese border ranges indicate that several brittle SW-directed thrusts are found SW and SE of Tal Nuur bounding small uplifted ridges (Fig. 14a). These are the only clear Cenozoic structures identified.

Qu and Zhang (1994) presented a cross section from near the Mongolian–Chinese border to the Junggar Basin (Fig. 1) which links with our study. They identified at least six major SW-directed brittle thrust faults in the Chinese Altai which they

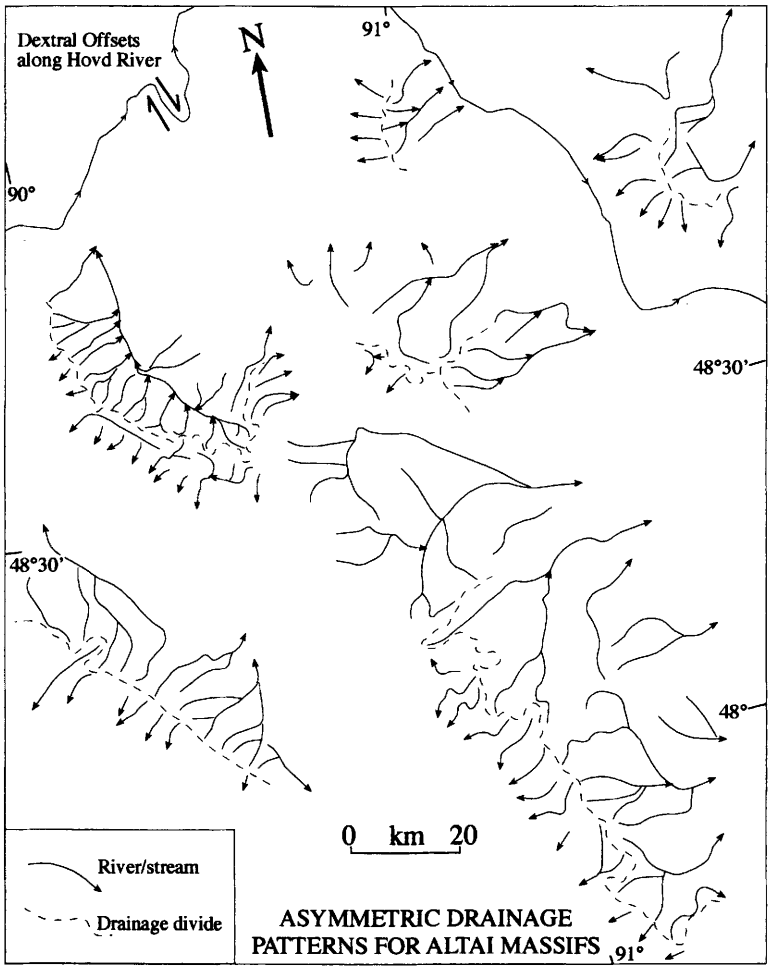

Fig. 15. River patterns for major block uplifts, northwestern Altai. Area shown is same as Figures 3, 4. Dextral offsets of Hovd River along Chikhtein Fault are indicated and visible in Figure 3.

argue are Palaeozoic in origin, but which were reactivated in the Cenozoic. Unfortunately, detailed evidence for Cenozoic reactivation was not provided. We are unaware of any modern studies investigating the Cenozoic construction of the Chinese Altai.

Discussion

In all areas studied, major Cenozoic thrust faults are SW-directed and bound the SW sides of major block uplifts. These faults are commonly transpressional segments of major regional dextral strike-slip faults or are commonly thrusts linked to them. Block uplifts have markedly asymmetric drainage patterns consistent with NE tilting due to SW-directed thrusting along SW range fronts (Figs 15, 16). Areas between active faults are geomorphologically mature and lack evidence for Cenozoic tectonic activity (Figs 3, 11). Thus Cenozoic deformation in the Altai is limited to discrete zones of Cenozoic reactivation (Fig. 17). The cross-strike Cenozoic architecture of the range at this latitude is relatively simple in that each range is essentially a large NE-tilted thrust block.

The Palaeozoic structural grain of basement metamorphic rocks in the region is generally NW-striking and NE-dipping. In numerous cases, we observed evidence for brittle reactivation of ductile shear zones and metamorphic fabric. It appears

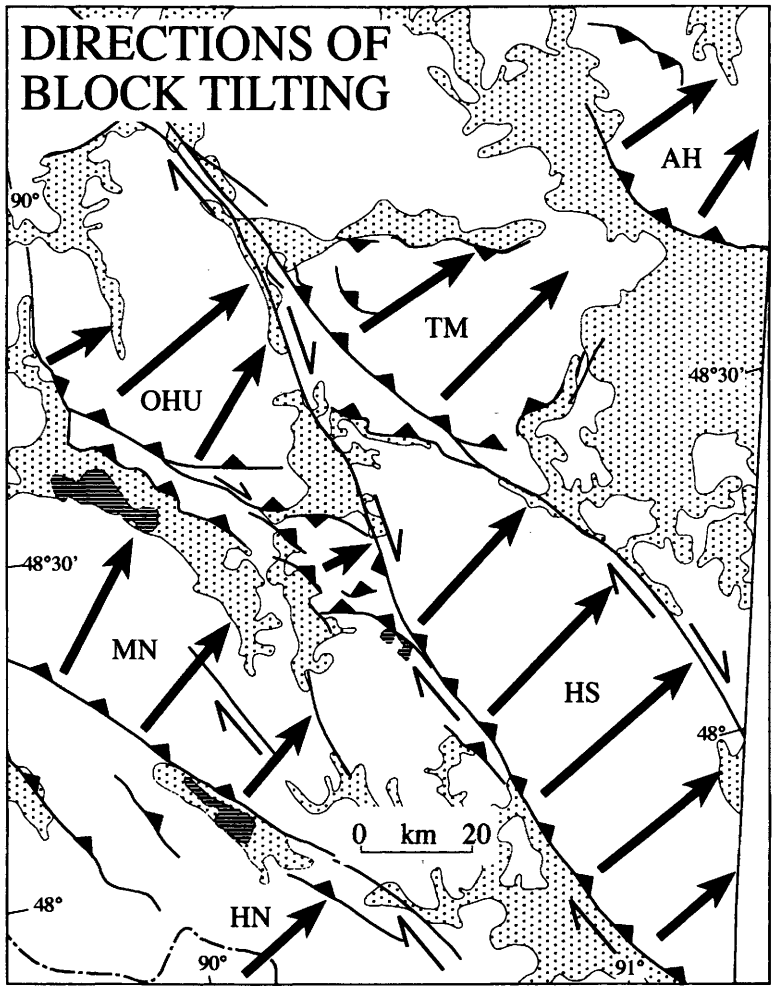

Fig. 16. Directions of bulk tilting for different Cenozoic uplifted blocks, northwestern Altai. Area shown is same as Figure 4. Directions of tilting are interpreted from drainage patterns (Fig. 15) and geometry of SW-directed Cenozoic thrust faults which bound major ranges in region. NE tilts are predominant. AH: Altun Huhey Uul; TM: Tsambagarav Massif; OHU: Omno Hayrhan Uula; HS: Hoh Serhiyn Nuruu; MN: Mengildyk Nuruu; HN: Hayrt Nuruu.

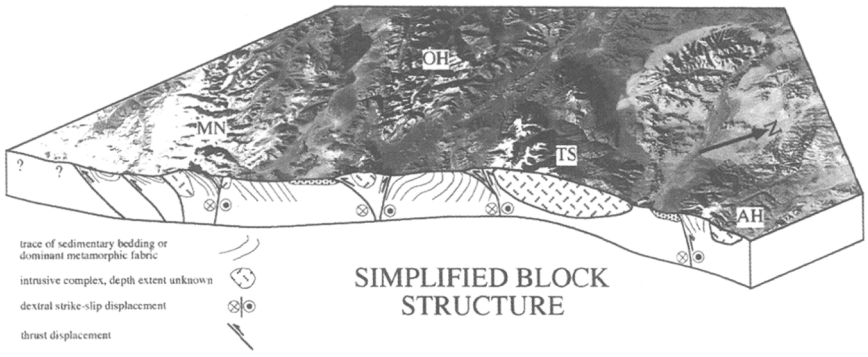

Fig. 17. Interpreted Cenozoic block structure of Mongolian Altai from Valley of Lakes SW to Chinese border. Attitude of basement fabrics is from unpublished field data by authors. AH: Altun Huhey Uul; TS: Tsambagarav Uul; OH: Omno Hayrhan Uula; MN: Mengildyk Nuruu.

likely that at first order, Cenozoic dextral transpressional reactivation of the Altai was controlled by this fundamental basement anisotropy. This has also been suggested for the Chinese Altai (Qu & Zhang 1994).

If the two-dimensional cross-strike architecture of the Altai appears relatively simple at the latitude of this study, the three-dimensional architecture is not. Each major range is a transpressional culmination with different strike-slip, oblique-slip, and thrust fault linkages (Fig. 18). Sair Uul is a flower structure pop-up between divergent splays of the Hoh Serkh Fault (Figs 3, 11). Altun Huhey Uul is a partial restraining bend that appears to accommodate most of the strike-slip motion of the Hovd Fault by thrusting along the SW mountain front; however, there is evidence that the fault also bypasses the range and continues towards the NE (Fig. 6b). The Jargalant range, which is the easternmost range of the Altai, SE of Altun Huhey Uul (Figs 2, 18), appears to be a more complete terminal restraining bend (cf. Cunningham *et al.* 1996). The Tsambagarav range is located at a gentle bend along the Ar Hötöl/Chikhtein Fault where there is a major component of compression and reverse displacement (Figs 3, 4). The triangular shape to the range is defined by bounding thrust faults and may be the result of southward propagation of the Chikhtein Fault and northward propagation of the Ar Hötöl Fault with the Tsambagarav

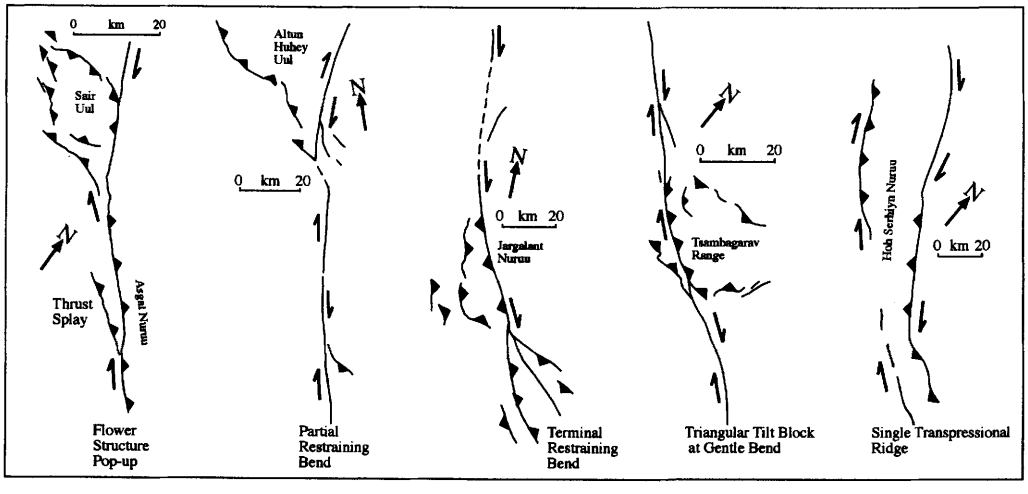

Fig. 18. Fault geometries of active transpressional culminations in Mongolian Altai including terminal restraining bends (Jargalant Nuruu), semi-terminal restraining bends (Altun Huhey Uul), triangular tilt blocks (Tsambagarav Massif), asymmetric flower structures between divergent splays (Sair Uul), and oblique-slip ridges (Hoh Serhiyn Nuruu).

range forming in the overlap/accommodation zone for the two fault systems (Fig. 18). The Hoh Serhiyn range is an elongate transpressional range with dextral and thrust components of displacement along both NE and SW sides. Asymmetric drainage patterns and overall topography suggest that the NW end of the range has greater thrust displacements along its SW margin, whereas the SE end of the range has experienced greater thrust displacements along its NE margin (Fig. 18).

The manner in which dextral strike-slip displacements are transferred to terminal thrusts and oblique-slip faults is complex and varies between individual ranges. In most ranges (Sair Uul, Altun Huhey Uul, Tsambagarav range), thrust faults die out away from linking strike-slip faults indicating a decrease in thrust displacement away from the fault junction. This suggests that the upthrusted block rotated around a vertical axis during displacement transfer (Bayasgalan *et al.* 1999).

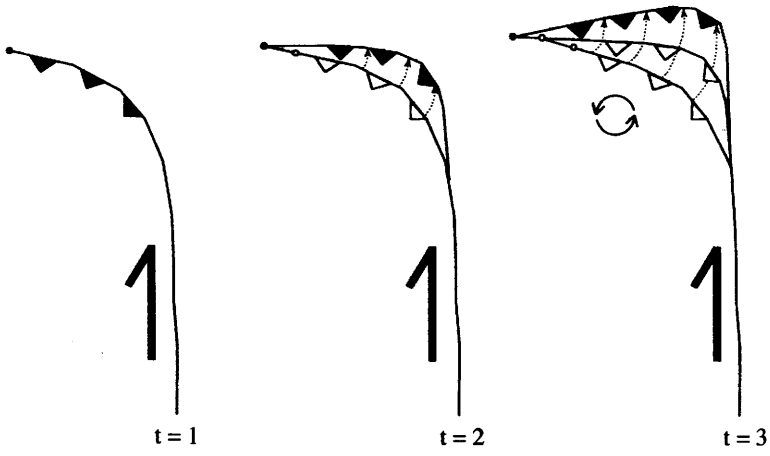

Fig. 19. Mechanism for block rotations through time (t=1 to t=3) at the termination zones for dextral strike-slip faults in the Mongolian Altai. Where the terminal thrust fault moves in the direction of strike-slip displacement (top example), the upthrusted block rotates in a counterclockwise sense with thrust displacement decreasing away from the junction between the thrust fault and strike-slip fault. This is interpreted to have occurred in the Tsambagarav range when viewed from NW to SE and may explain the triangular shape of the range (Figs 3, 4, 18). Where the terminal thrust fault moves in a direction opposite to the strike-slip sense, the upthrusted block rotates in a clockwise sense and the thrust fault propagates down the length of the strike-slip fault overriding it. This is interpreted to have occurred along the SW front of the Mengildyk Nuruu range (Tal Nuur thrust) when viewed from the SE (Figs 3, 4).

Rotation is presumably greatest where the fault intersection angle is highest and the thrust offset is largest. However, the sense of block rotation is dependent on whether the linking thrust moves forward in the same direction as the strike-slip motion or whether it moves in an opposite sense (Fig. 19). For example, thrusts at the southern end of the Tsambagarav range have moved SE indicating counterclockwise rotation through time (Figs 18, 19). Conversely, the Tal Nuur thrust is interpreted to have rotated in a clockwise sense with time to the point where the linking strike-slip fault at the southern end of the Mengildyk Nuruu range is almost completely overridden (Fig. 19).

A block rotation mechanism for accommodation of Late Cenozoic strike-slip fault displacements is documented by palaeomagnetic data in the Russian Altai, 400 km north of the region studied here (Thomas *et al.* 1998; Bayasgalan *et al.* 1999). Unfortunately, to our knowledge, there are no published palaeomagnetic data for anywhere in the Mongolian Altai, so the amount of block rotation within the Mongolian Altai is unconstrained. We think it is also likely that the regional strike-slip faults within the Mongolian Altai have rotated with the blocks they bound. Counterclockwise rotation of originally more N–S-trending strike-slip faults to more NW-trending orientations would have reoriented the faults more favourably for contractional deformation and might explain why faults like the Hoh Serkh Fault have important reverse components of motion and have nucleated discrete thrust splays along their lengths such as the Tsagaan Salaa thrust (Figs 11, 18). In summary, we believe that the Mongolian Altai is a superb natural laboratory for studying a diverse range of actively forming and interlinking transpressional fault systems with associated block rotations.

Structural evidence from the Chinese Altai adjacent to the area studied here indicates that the range is dominated by a NW-striking moderate- to low-angle thrust belt that overthrusts the Junggar Basin to the SW (Qu & Zhang 1994). These faults are reported to be Palaeozoic thrusts that have been reactivated in the Late Cenozoic. We see little evidence on satellite images of the Chinese Altai that the thrust faults are linked with regional strike-slip faults as is found in the Mongolian Altai. Thus it appears that at the latitude studied here, the Altai is fundamentally partitioned into a low-angle thrust belt that overthrusts the Junggar Basin on the Chinese side, and a high-angle dextral transpressional belt on the Mongolian side (Fig. 20). Structural vergence is consistently towards the SW across the entire range.

Elsewhere along strike, Cenozoic structural vergence may not be entirely to the SW. For example, Cunningham *et al.* (1996) reported coalesced parallel flower structures in the southernmost Altai which contain Cenozoic thrust faults with both SW and NE vergence. Our recent field results from areas 100 km south of the region studied here also indicate that some major Cenozoic thrusts are NE directed, towards the Valley of Lakes. Clearly, more work is needed throughout the range to better understand along-strike changes

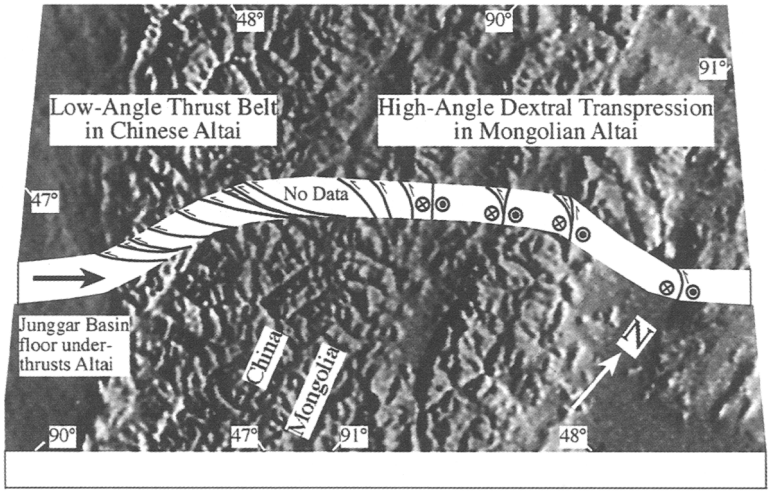

Fig. 20. Simplified section across Altai incorporating data from this study and information in Qu & Zhang (1994). Mongolian Altai is dominated by dextral transpressional block uplifts and high-angle faults whereas the Chinese Altai is characterized by a low-angle thrust belt that overthrusts the Junggar Basin. Cenozoic structural vergence along this line is dominantly towards the SW.

in Cenozoic fault geometry and crustal architecture.

There appear to be three fundamental controls on why Cenozoic mountain building in the Altai region is dominated by dextral transpression: (1) NE–SW-directed SHmax due to India's continued NE indentation (Zoback 1992), (2) pre-existing NW–SE crustal anisotropy in mechanically weak metasedimentary and metavolcanic basement rocks, and (3) the presence of rigid crustal blocks underlying the Hangay and Junggar Basin regions which have resisted internal deformation, but have focused deformation in the Altai between the two blocks. The Hangay region is believed to be underlain by a mechanically rigid Precambrian cratonic block (Cunningham 2001). This is based on Archaean–Neoproterozoic zircon ages on basement rocks and middle–late Precambrian Sm–Nd model ages for granites throughout a wide area (Kovalenko *et al.* 1996). The outline of the Hangay Block is well defined on aeromagnetic maps of Mongolia (Fig. 21). We view the Hangay Block as

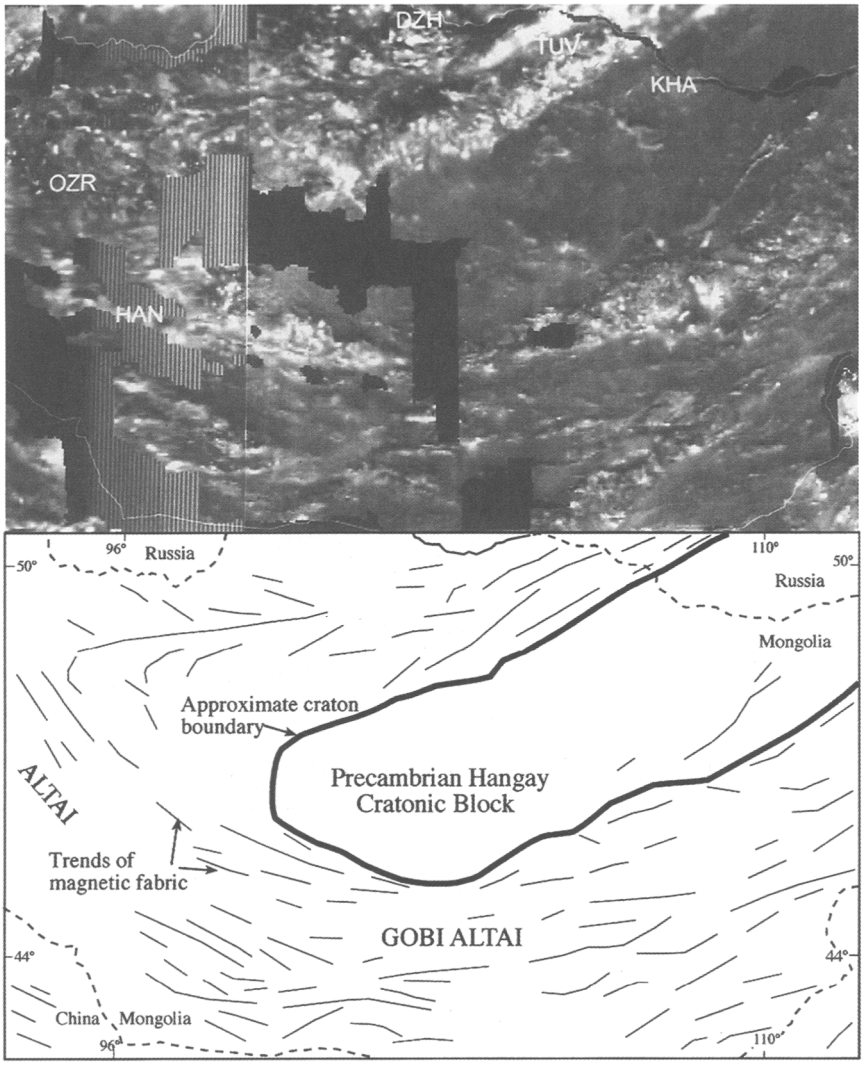

Fig. 21. Unpublished aeromagnetic map of Mongolia courtesy of Mongolian Academy of Sciences, Institute of Geology and Mineral Resources. Despite areas of missing data, regional structural trends and outline of Hangay Precambrian block are well defined. Acronyms are in Russian on original map (DZH = Dzhida Belt in northern Mongolia, OZR = Valley of Lakes, KHA = Hangay Block, HAN = Han Tayshir ophiolite occurrence in southern Valley of Lakes).

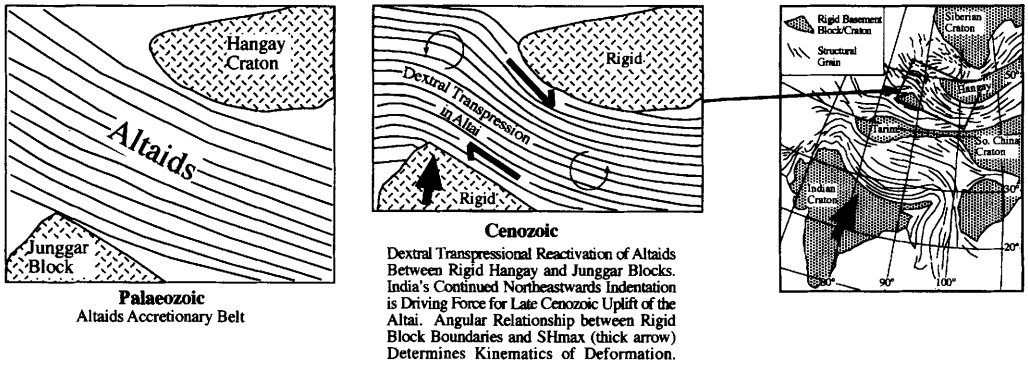

Fig. 22. Cartoon depicting Altai as weak Palaeozoic accretionary belt sandwiched between more rigid Junggar Block and Hangay Precambrian cratonic block. Continued Tertiary indentation of India drives Junggar Block northwards. Hangay craton acts as passive indentor and Altai belt is reactivated in dextral transpression between rigid blocks. Counterclockwise rotation of northern and southern ends of Altai is driven by NE-directed SHmax and geometry of rigid block boundaries.

a passive indentor which has focused late Cenozoic deformation around its W, SW and S margins in the Altai and Gobi Altai (Cunningham 2001).

The age and composition of the Junggar Basin basement are unknown. The crust is mechanically strong with an unusually high elastic thickness (T_e ~35 km; Maggi *et al.* 2000). The high strength of the Junggar Basin crust may be due to an earlier history of Permian rifting which resulted in basaltic intrusion and underplating (Allen *et al.* 1991; M. Allen, pers. comm. 2001). What is clear is that along the southern and NE margins of the Junggar Basin Block, Cenozoic mountain building is actively occurring, whereas the basin interior has resisted deformation. Figure 22 is a simplified model showing how dextral transpression in the Altai region is linked to the larger deformation field of Central Asia. The model suggests that as the Junggar Basin Block is displaced northwards with respect to the relatively fixed Siberian and Hangay cratons, the Altai region basement is reactivated in dextral transpressional mode parallel to the pre-existing basement grain. The angular relationship between the rigid block boundaries and SHmax determines the kinematics of deformation. With continued northwards displacement (indentation) of the Junggar Block, counterclockwise rotation of the northern and southern ends of the Altai occurs and is expressed in the gentle oroclines that are found at opposite ends of the range (Fig. 1).

We are grateful to British Petroleum for providing satellite imagery. Thanks to Tsogo, Zoloo, Otgon and Tunga for assistance in the field. This project was funded by National Geographic Society Committee for Research and Exploration Grant 6308–98 to W. D. Cunningham. A. Dijkstra was supported by a European Commission Marie Curie Fellowship.

References

ALLEN, M. B., WINDLEY, B. F., CHI, Z., ZHONG-YAN, Z. & GUANG-REI, W. 1991. Basin evolution within and adjacent to the Tien Shan Range, NW China. *Journal of the Geological Society of London,* **148**, 369–378.

BALJINNYAM, I., BAYASGALAN, A. *et al.* 1993. *Ruptures of Major Earthquakes and Active Deformation in Mongolia and its Surroundings*. Geological Society of America Memoir, **181**.

BAYASGALAN, A., JACKSON, J., RITZ, J. -F. & CARRETIER, S. 1999. Field examples of strike-slip fault terminations in Mongolia and their tectonic significance. *Tectonics,* **18**(3), 394–411.

CUNNINGHAM, W. D. 1998. Lithospheric controls on late Cenozoic construction of the Mongolian Altai. *Tectonics,* **17**(6), 891–902.

CUNNINGHAM, W. D. 2001. Cenozoic normal faulting and regional doming in the southern Hangay region, Central Mongolia: implications for the origin of the Baikal rift province. *Tectonophysics,* **331**, 389–411.

CUNNINGHAM, W. D., WINDLEY, B. F., DORJNAMJAA, D., BADAMGAROV, G. & SAANDAR, M. 1996. Structural transect across the Mongolian Altai: active transpressional mountain building in central Asia. *Tectonics,* **15**(1), 142–156.

DEVYATKIN, E. V. 1974. Structures and formational complexes of the Cenozoic activated stage. *In*: *Tectonics of the Mongolian People's Republic*. Moscow, Nauka, 182–195 (in Russian).

HENDRIX, M. S., GRAHAM. S. A., CARROLL, A. R., SOBEL, E. R., MCKNIGHT, C. L., SCHULEIN, B. J. & WANG, Z. 1992. Sedimentary record and climatic implications of recurrent deformation in the Tien Shan: evidence from Mesozoic strata of the north Tarim, south Jung-

gar, and Turpan basins, northwest China. *Geological Society of America Bulletin,* **104**, 53–79.

HOWARD, J. P., CUNNINGHAM, W. D., DAVIES, S. J., DIJKSTRA, A. H. & BADARCH, G. (in press). The stratigraphic and structural evolution of the Dzereg Basin, Western Mongolia: clastic sedimentation, fault inversion and basin destruction in an intracontinental transpressional setting. *Basin Research.*

KHIL'KO, S. D., KURUSHIN, R. A., KOCHETKOV, V. M., BALJINNYAM, I. & MONKOO, D. 1985. *Earthquakes and the Bases for Seismic Zoning of Mongolia.* Transactions 41, The Joint Soviet–Mongolian Scientific Geological Research Expedition, Moscow, Nauka.

KOVALENKO, V. I., YARMOLYUK, V. V., KOVACH, V. P., KOTOV, A. B., KOZAKOV, I. K. & SALNIKOVA, E. B. 1996. Sources of Phanerozoic granitoids in Central Asia: Sm–Nd isotope data. *Geochemistry International,* **34**, 628–640.

MAGGI, A., JACKSON, J. A., MCKENZIE, D. & PRIESTLEY, K. 2000. Earthquake focal depths, effective elastic thickness, and the strength of the continental lithosphere. *Geology,* **28**(6), 495–498.

Mongolian National Atlas 1990. Ulaan Baatar, Moscow.

QU GUOSHENG & CHONG MEIYING 1991. Lead isotope geology and its tectonic implications in the Altaides, China. *Geoscience,* **5**, 100–110.

QU GUOSHENG & ZHANG JINJIANG 1994. Oblique thrust systems in the Altay orogen, China. *Journal of Southeast Asian Earth Sciences,* **9**(3), 277–287.

SENGÖR, A. M. C. & NATAL'IN, B. A. 1996. Paleotectonics of Asia: fragments of a synthesis. *In*: YIN, A. & HARRISON, T. M. (eds) *The Tectonic Evolution of Asia.* Cambridge University Press, 486–640.

SENGÖR, A. M. C., NATAL'IN, B. A. & BURTMAN, V. S. 1993. Evolution of the Altaid tectonic collage and Palaeozoic crustal growth in Eurasia. *Nature,* **364**, 299–307.

SJOSTROM, D. J. 1997. *Lower–Middle Jurassic through Lower Cretaceous sedimentology, stratigraphy and tectonics of Western Mongolia.* MSc thesis, University of Montana.

TAPPONNIER, P. & MOLNAR, P. 1979. Active faulting and Cenozoic tectonics of the Tien Shan, Mongolia, and Baykal regions. *Journal of Geophysical Research,* **84**, 3425–3459.

THOMAS, J. C., LANZA, R. KAZANSKY, A., ZYKIN, C. V. S., SEMAKOV, N., MITROKHIN, D. & DELVAUX, D. 1998. Paleomagnetic study of Cenozoic sediments in the Siberian Altai and the Zaisan Basin, central Asia: evidence for heterogeneous vertical axis rotations during the Tertiary (abstract). *In*: DOBRETSOV, N. L., KLERKX, J. & LOGATCHEV, N. L. (eds) *Active Tectonic Continental Basins.* University Gent, Belgium, 67.

TRAYNOR, J. J. & SLADEN, C. 1995. Tectonic and stratigraphic evolution of the Mongolian People's Republic and its influence on hydrocarbon geology and potential. *Marine and Petroleum Geology,* **12**, 35–52.

TRIFONOV, V. G. 1988. Mongolia – an intracontinental region of predominantly recent strike-slip displacement: active faults. *In*: *Neotectonics and Contemporary Geodynamics of Mobile Belts.* Moscow, Nauka, 239–272 (in Russian).

WEBB, L. E., GRAHAM, S. A., JOHNSON, C. L., BADARCH, G. & HENDRIX, M. S. 1999. Occurrences, age, and implications of the Yagan-Onch Hayrhan metamorphic core complex, southern Mongolia. *Geology,* **27**, 143–146.

ZAITSEV, N. S. 1978. *Geological Map of the Mongolian Altai, 1:500,000 Scale.* Acad. Sci. USSR, Acad. Sci. Mongolian People's Republic, Comb. Sov.–Mongolian Sci. Res. Geol. Exped. Nauka, Moscow (in Russian).

ZOBACK, M. L. 1992. First- and second-order patterns of stress in the lithosphere: the world stress map project. *Journal of Geophysical Research,* **97**(B8), 11703—11728.